Circulating endothelial progenitor cells are involved in VEGFR-2-related endothelial differentiation in glioma

LE WANG[1*], LU CHEN[2*], QIANFENG WANG[2], LIJUAN WANG[1], HAIBAO WANG[1], YUJUN SHEN[2], XIAOHU LI[1], YU FU[2], YUXIAN SHEN[2] and YONGQIANG YU[1]

[1]Department of Radiology, The First Affiliated Hospital, Anhui Medical University, Hefei, Anhui 230022; [2]Biopharmaceutical Research Institute, School of Basic Medical Sciences, Anhui Medical University, Hefei, Anhui 230032, P.R. China

Received May 13, 2014; Accepted August 19, 2014

DOI: 10.3892/or.2014.3467

Abstract. Endothelial progenitor cells (EPCs) play important roles in maintaining endothelial integrity and tumor vascularization. However, the differentiation of EPCs in the neoangiogenesis of gliomas has not yet been fully elucidated. The purpose in this study was to investigate the profile of EPC differentiation in rat C6 glioma using magnetic resonance imaging (MRI), a non-invasive monitoring assay. To achieve this goal, we isolated EPCs from rat bone marrow and identified them by detecting CD34, CD133, and VEGFR-2, the markers of EPCs. Coexpression of Ac-LDL and UEA-1 in EPCs was also determined. To dynamically monitor the migration of circulating cells, the EPCs were labeled with ultrasmall superparamagnetic iron oxide (USPIO) and injected by tail vein into rats bearing C6 glioma. MRI was performed at 24, 48, and 96 h after injection. The distribution and differentiation of EPCs were confirmed by histology. We found that the USPIO-labeled EPCs appeared at the tumor periphery where a large number of CD105-positive cells appeared at 24 h after injection by using MRI scanning. Ninety-six hours after injection, immunohistochemistry and Prussian blue staining were used to observe the labeled EPCs in the tumor tissue. We found that many of the labeled EPCs were overlapped with VEGFR-2-positive endothelial cells, but not CD105- or CD34-positive cells. These results suggest that EPCs can cross the blood-brain barrier from peripheral blood and home to tumors, where they differentiate into endothelial cells, including VEGFR-2-positive endothelial cells. MRI is a useful method for dynamically tracking the migration of USPIO-labeled EPCs.

Correspondence to: Dr Yongqiang Yu, Department of Radiology, The First Affiliated Hospital, Anhui Medical University, Hefei, Anhui 230022, P.R. China
E-mail: yuyongqiang@hotmail.com

Dr Yuxian Shen, School of Basic Medical Sciences, Anhui Medical University, Hefei, Anhui 230032, P.R. China
E-mail: shenyx@ahmu.edu.cn

*Contributed equally

Key words: endothelial progenitor cells, glioma, magnetic resonance imaging, ultrasmall superparamagnetic iron oxide, VEGFR-2

Introduction

Endothelial progenitor cells (EPCs) are the precursor cells of vascular endothelial cells. The specific surface marker of EPCs for identification is CD133, which is a subpopulation of $CD34^+$ hematopoietic stem cells. In 1997, EPCs were first isolated from human peripheral blood (1). Since then, strong evidence has been found concerning EPCs in bone marrow, cord blood, and peripheral blood (2-5). EPCs can adhere to the endothelium at the zones of ischemic or hypoxic tissue to repair vascular intima and participate in new vessel formation, suggesting that EPCs play an important role in maintaining endothelial integrity and tumor vascularization (6-12). EPCs can home to tumor tissues for tumor vascularization, which depends on stimuli from the target tissue and the ability of the resident bone marrow population to respond (13,14). Recently it was reported that EPCs are increasingly mobilized in patients with malignant gliomas, and their levels correlate with tumor angiogenic activity (15). Due to the association with tumors, EPCs are considered as a gene carrier/delivery system for glioma therapy as well as imaging probes (16). However, the role of EPCs in the neoangiogenesis of gliomas has not yet been fully elucidated. Recently, Corsini *et al* found that there was no relationship between VEGF plasma levels and EPCs in glioma patients (17). Soda *et al* reported that EPCs mobilized from bone marrow could initiate angiogenesis through release of paracrine factors rather than structurally incorporating into the vessel wall (18). We wished to elucidate the cell type that EPCs differentiate to in tumor tissue. To achieve this goal, we isolated EPCs from rat bone marrow and identified them by detecting markers of EPCs. The EPCs were labeled with ultrasmall superparamagnetic iron oxide (USPIO) and were injected by the tail vein into rats with brain C6 glioma. Magnetic resonance imaging (MRI) was performed to dynamically track EPC migration. The distribution and differentiation of the EPCs were confirmed by histology.

Materials and methods

Materials. Adult Sprague-Dawley rats, weighing ~100 g (for cell extraction procedures) or 300 g (for animal models), were obtained from the Animal Center of Anhui Province (no. SCXK-Wan-2005-001). All animals were fed with a standard laboratory diet and tap water in a temperature- and humidity-controlled animal house under a 12-h light-dark cycle. All of the procedures were performed according to the Guidelines of the Animal Care and Use Committee of Anhui Medical University, which is in accordance with the National Institute of Health Guide for the Care and Use of Laboratory Animals. All of the experimental procedures were approved by the Ethics Committee of Anhui Medical University for Animal Experimentation.

The reagents and instruments were as follows: USPIO (Guerbet, France); EGM-2 medium (Lonza, Switzerland); rabbit polyclonal anti-CD133 (ab16518) and mouse monoclonal anti-VEGFR-2 (ab9530) (Abcam, England); mouse monoclonal anti-CD105 (Millipore, Germany); mouse monoclonal anti-CD34 (Santa Cruz, USA); Dil-labeled acetylated low density lipoprotein (Dil-Ac-LDL; Invitrogen, USA); FITC-labeled *Ulex europaeus* agglutinin 1 (FITC-UEA-1; Sigma, USA); poly-l-lysine (PLL; Sigma, USA); 3.0 T Signa HDxt MR system (GE Healthcare, Milwaukee, WI, USA) and lymphocyte separation medium (TBD, China).

Cell culture and identification. The cells, extracted from rat bone marrow by density centrifugation with lymphocyte separation medium, were cultured in EGM-2 medium at 37˚C, in a 95% air, 5% CO_2 atmosphere. The culture medium was replaced every 4 days. After a 14-day culture, the secondary generation cells were identified for EPCs by immunohistochemical and immunofluorescent staining with the surface markers CD133, CD34 and VEGFR-2.

Labeling of EPCs with USPIO. USPIO and PLL (used as a transfection agent) were mixed in a tube containing serum-free EGM-2 medium and were then incubated for 60 min at room temperature (19). The final concentrations of USPIO and PLL were 25 and 0.5 μg/ml, respectively. The USPIO-PLL mixture was added directly to the cells, and the samples were incubated for 1, 3 and 5 days, respectively.

Staining for intracellular iron. After incubation with USPIO-PLL, the Prussian blue (PB) assay was used for the detection of iron particles in the cells. After washing and fixation, the labeled cells were stained for the presence of intracellular iron with freshly prepared Pearls' reagent solution (mixture of equal volumes of 2% potassium ferrocyanate and 6% hydrochloric acid) for 30 min. After washing three times with distilled water, the cells were counterstained with Nuclear Fast Red at room temperature for 5 min.

Cell viability. The MTT assay was used for detecting cell viability. The absorbance of the formazan product was then measured at a wavelength of 490 nm. Before the MTT assay, the labeled and unlabeled EPCs were exposed to 0.4% trypan blue dye, and the ratio of non-stained viable cells was calculated.

In vitro MRI of the labeled EPCs. A 0.4-ml aliquot of 1% agarose was added into a 0.5-ml EP tube. After digestion with trypsin, the cells were rapidly mixed with 100 μl of an 8% gelatin solution at concentrations of $2x10^6$, $1x10^6$, $5x10^5$ and $2.5x10^5$ cells/ml at 37˚C, and then added into the EP tubes. To avoid susceptibility artifacts from the surrounding air, all tubes were placed in water after cooling. The clinical 3.0 T MR scanner and the laboratory coil for animals were used to detect the signal of the labeled EPCs. Multi-echo spin-echo sequence (T2 map) (TR/TE = 2000/8.3, 16.6, 24.9, 33.2, 41.5, 49.8, 58.1, 66.5 msec, band width = 41.7 kHz, FOV = 9 cm x 9 cm, slice thickness = 1 mm) and multi-gradient-echo sequence (T2* map) (TR = 120 msec, TE = 2.7, 7.1, 11.5, 15.9, 20.3, 24.7, 29.1, 33.5 msec, band width = 31.25 kHz, flip angle = 30˚, FOV = 9 cm x 9 cm, slice thickness = 1 mm) were used. The correlation between the concentrations of the labeled cells and the $R2/R2^*$ values was compared.

Animal model. C6 cells (Institute of Biochemistry and Cell Biology, SIBS, CAS) were incubated in DMEM supplemented with 10% fetal bovine serum at 37˚C, in 5% CO_2. For implantation, C6 cells were trypsinized and resuspended at a concentration of $1x10^7$ cells/ml. The head of the rat was fixed on a stereotactic apparatus after being anaesthetized with 10% chloral hydrate (0.3 ml/100 g). It was ensured that the anterior fontanelle and the andalusite occipital fontanelle of the rat were in the same plane. The coordinates used for the injection site were 1 mm from the anterior arcuate suture, 3 mm to the right of the sagittalis suture, and 5 mm deep. A 10 μl amount of the cell suspensions was injected into the brain with a speed of 1 μl/min.

Implantation of the labeled EPCs. Seven days after C6 cell injection, all of the rats were scanned with plain and contrast-enhanced (Gd-DTPA, 0.1 mg/kg) MRI. This allowed assessment of glioma tumor size. When the tumors were ~3 to 5 mm, the USPIO-labeled EPCs were injected into the tail vein. Before tail vein injection, the USPIO-PLL labeled EPCs were collected, washed twice with sterile phosphate-buffered saline (PBS), resuspended at a concentration of $5x10^6$ cells/ml with serum-free EBM-2 culture medium. Tumor-bearing rats were randomly divided into two groups and intravenously injected with labeled cells (n=10) or non-labeled cells (n=4), respectively. Each rat was injected by the tail vein with 1 ml of the cell suspensions.

In vivo MRI experiments. The rats were anaesthetized with 10% chloral hydrate (0.3 ml/100 g) and scanned with MRI at different time points (1, 2, 4 and 7 days after EPC injection). MRI images were obtained using a 3.0-Tesla MRI system, with an animal coil (inner diameter = 3 inch). Axial images over the head were acquired with an 8.0-cm-square field of view (FOV), and a 2.5-mm slice thickness. Scans were performed using fast spin echo T2-weighted (TR = 2000 msec, TE = 46 msec), T1-weighted (TR = 400 msec, TE = 9.5 msec), and $T2^*$map (TR = 120 msec, TE = 2.8-35.4 msec) sequences.

Histological analysis. After the *in vivo* MRI experiments, the brain tissues (including the tumor) were fixed with 4% paraform, and then embedded in paraffin. Coronal sections (5 μm) were processed for Prussian blue staining

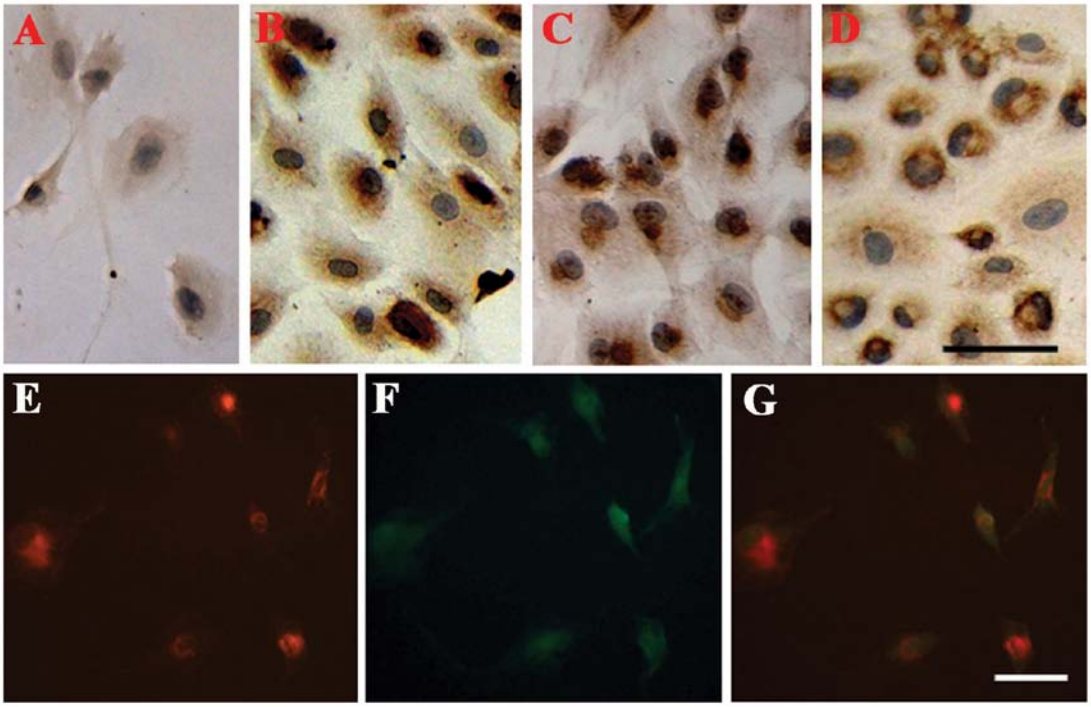

Figure 1. Identification of EPCs. The cells, isolated from rat bone marrow, were passaged to the second generation and identified using anti-VEGFR-2 (B), anti-CD133 (C) and anti-CD34 (D) antibodies. The negative control for the immunohistochemistry assay was performed by replacing the primary antibodies with PBS (A). DiL-Ac-LDL (E, red), an endothelial marker, was double labeled with FITC-tagged UEA-1 (F, green). The merged images of (E) and (F) was presented in (G). Scale bar, 50 μm.

and immunohistochemistry using standard procedures. The sections were incubated with the primary antibody overnight at 4˚C. Negative controls were performed by substituting the primary antibody with PBS. The primary antibodies used in this study included mouse anti-CD105, anti-CD34, and KDR1 (VEGF receptor 2) antibody.

Immunofluorescence staining. The EPCs seeded on coverslips were fixed with 4% paraformaldehyde, permeabilized in 0.1% Triton X-100, blocked by 1% BSA, and stained with the indicated primary antibodies followed by fluorescent secondary antibodies. Negative controls were performed by substituting the primary antibody with PBS. Nuclei were counterstained with DAPI (Sigma).

Statistical analysis. The data are presented as mean ± SD. Statistical significance of the results was analyzed using the χ^2 test and analysis of variance. $P<0.05$ was considered to indicate a statistically significant difference.

Results

Preparation and identification of EPCs. The cells were isolated from rat bone marrow and cultured in EGM-2 medium. After 14 days, they were passaged to the second generation and identified with EPC markers: VEGFR-2, CD133 and CD34. We found that most of the EPCs revealed positive immunoreactivity for VEGFR-2 (Fig. 1B), CD133 (Fig. 1C) and CD34 (Fig. 1D) antibody, respectively. Dil-c-LDL (Fig. 1E, red), an endothelial marker, was detected to co-localized with UEA-1 (Fig. 1F, green) in the EPCs. These results suggest that we successfully obtained EPCs.

Labeling of EPCs with UPSIO and evaluation of the viability. In the magnetically labeled EPCs, we found a large number of blue particles in the cytoplasm (Fig. 2B). The labeling efficiencies were increased along with the prolongation of culture time. No blue particle was observed in the control cells (non-labeled cells, Fig. 2A). There was no significant change in cell viability as detected by trypan blue dye exclusion assay. The viability of both the labeled and non-labeled cells was >95%. The MTT assay showed that there was no significant difference in cell proliferation between the two groups (data not shown). These results suggest that the magnetic marker USPIO had no effect on the cell vitality.

In vitro MRI of the USPIO-labeled EPCs. The relationship between the concentration of the USPIO-labeled cells and the R2/R2* values on the T2 and T2* map sequences is shown in Fig. 2C-E. The results indicated that the relaxation time on the T2* map was significantly lower than that on the T2 map for the same cell concentration (Fig. 2C). A linear correlation was found between the cell concentrations and the R2 or R2* values. The linear slope corresponding to the effects of R2 and R2* was 3.186×10^{-4} and 11.409×10^{-4}, respectively (Fig. 2D and E). The effects of R2* were significantly larger than those of R2.

MR tracks the migration of the USPIO-labeled EPCs into the tumor periphery. Five days after the implantation of the C6 cells into the right basal ganglia, MRI was performed using T1-weighted, T2-weighted, Gd-DTPA enhanced scanning, and the additional T2* map sequence. We found small, well-circumscribed, point- or nodule-like lesions in the right basal ganglia in 9 rats among the 14 surviving rats, but 5 rats

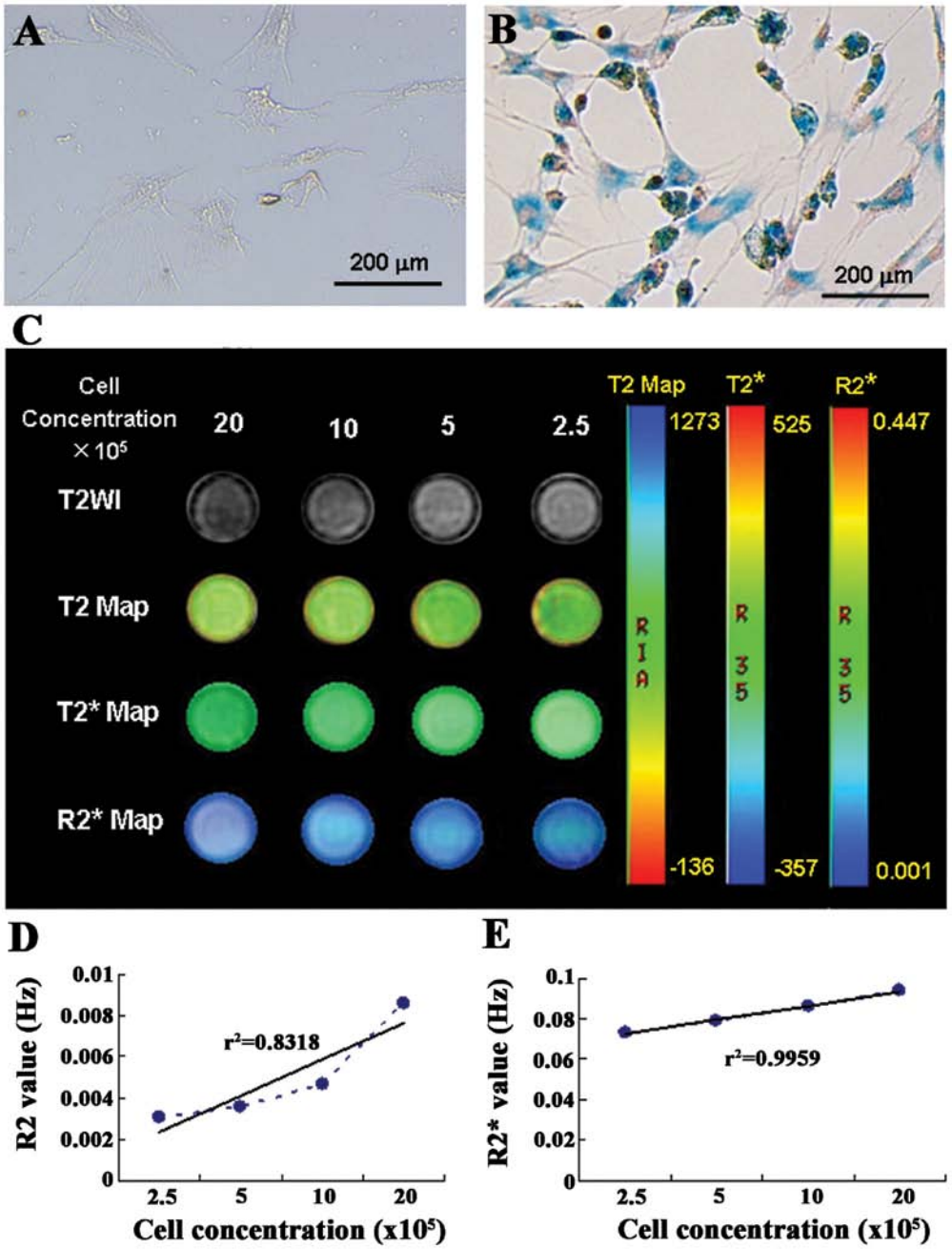

Figure 2. Labeling of EPCs with USPIO. The non-labeled EPCs (A) and USPIO-labeled EPCs (B) were stained with Prussian blue. Scale bar, 200 μm. (C-E) The relationship between the concentration of the USPIO-labeled cells and the R2/R2* values. (C) Map images of the labeled cells scanned with the indicated sequences. (D and E) Correlation between the cell concentrations and R2 values (D) or R2* values (E).

had no obvious lesions (Fig. 3B). These signals suggest the formation of a solid tumor. Due to the fact that the rat brain injuries induced by tumor implantation did not have enough time to heal (in a 5-day period), the line-like signals in most of the rat brains on the T2* map suggest the passage of the needle (Fig. 3C, indicated by the arrow).

Seven days after the implantation of the C6 cells, the labeled and unlabeled EPCs were intravenously injected into the rats through the tail vein. Twenty-four hours later, the rats were scanned at the indicated time points (Fig. 3D-L). The MRI results showed that the solid part appeared as a hyperintense signal on Gd-enhanced T1-weighted image at 24 h after the injection of the labeled cells (Fig. 3D). A low-intensity signal at the tumor periphery appeared on both the T2-weighted image and the T2* map (Fig. 3E and F), which was different from the passage of the needle in Fig. 4C. MR tracking at different time points demonstrated that the migration of the labeled EPCs into the tumor periphery appeared as a low signal intensity on both the T2-weighted and T2* map, especially on the T2* map. For the control group, a low signal was observed in the right basal ganglia where the needle had been inserted, and then the signal gradually faded away on the T2* map sequence (Fig. 3M-O). No significant difference was found between the signals from before and after the injection of the non-labeled EPCs.

USPIO-labeled EPCs are involved in the neovasculature of the tumors. After the *in vivo* MRI analysis, the tumor tissues

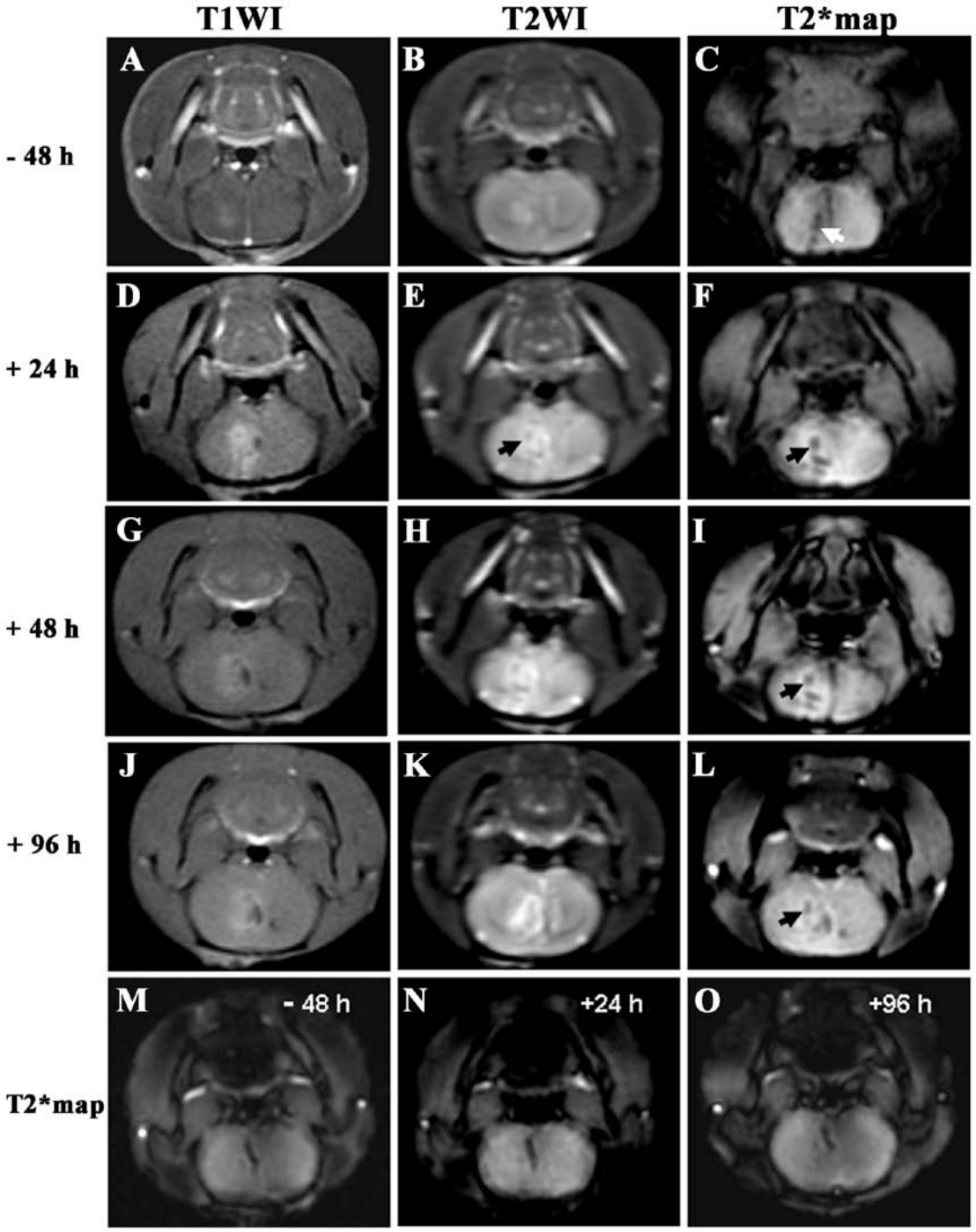

Figure 3. MRI tracks the USPIO-labeled EPCs *in vivo*. (A-C) Images collected at 48 h before injection of the labeled cells into the tail vein of the rats. The arrow shows the passage of the needle in the right basal ganglia for the C6 cell injection. (D-F) Images captured at 24 h after injection of the labeled cells. A low signal (arrow) presented at the margin of the tumor under T2-weighted image (E). The low signal was more significant on the T2* map (F). These low signals were different from the passage of the needle in panel C. The solid tumor appeared as hyperintensity Gd-enhanced under T1-weighted image (D). (G-I) Images captured at 48 h after injection of the labeled cells. (J-L) Images captured at 96 h after injection of the labeled cells. (M-O) T2-weighted images of the control group with non-labeled EPCs at the indicated time points.

were processed for Prussian blue staining and immunohistochemistry. Corresponding to the low signal areas at the margin of tumors in the MRI image (Fig. 4A), iron-positive cells appeared in this region (Fig. 4C and D), suggesting that the UPSIO-labeled EPCs might home to the tumor. The solid tumor tissue was verified by H&E staining (Fig. 4B). The consecutive sections of the paraffin-embedded tumor tissues were stained for EPCs using anti-CD105, anti-VEGFR-2 and anti-CD34. The results revealed that there were a large number of CD105-positive cells in the tumor tissues, particularly in the peripheral zone of the tumors (Fig. 4E and F), where many iron particles accumulated. A few CD34-positive cells were dispersed in the tumor tissue (Fig. 4G-I). More importantly, we found that some iron particles appeared in the VEGFR-2-positive cells when double labeled with Prussian blue and VEGFR-2 (Fig. 5E and F), but not CD105- (Fig. 5A and B) or

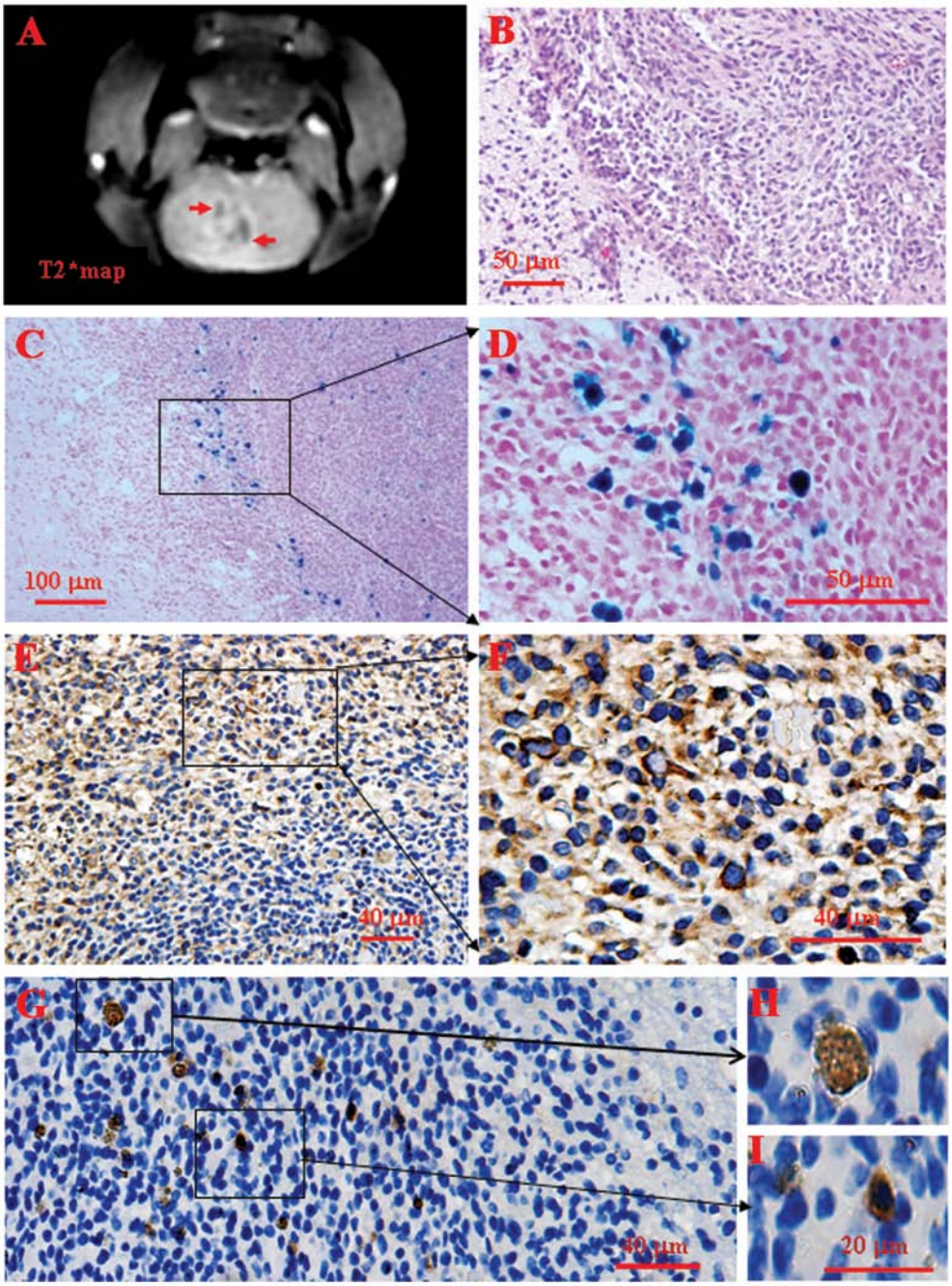

Figure 4. USPIO-labeled EPC incorporation into the neovasculature of the tumor. (A) MR image shows low signals (arrows) around the tumor on the T2* map. (B) Tumor tissue was stained by H&E. Scale bar, 50 μm. (C and D) Prussian blue staining shows the USPIO-labeled cells. Scale bar, 100 μm in C and 50 μm in D, respectively. (E and F) Expression of CD105 in the tumor tissue. Scale bar, 40 μm. (G-I) Expression of CD34 in the tumor tissues. Scale bars are as indicated.

CD34-positive cells (Fig. 5C and D). These results suggest that the USPIO-labeled EPCs were specifically transformed into VEGFR2-related endothelial cells in the tumors.

Discussion

EPCs refer to multiple cell types that differentiate into the endothelial lineage and express CD34, VEGFR-2 and CD133 on their surface. It has been widely accepted that EPCs can phagocytize acetylated-LDL and bind to lectin (UEA-1) (20,21). The uptake of Dil-Ac-LDL is an assessment of differentiated EPCs. In the present study, we found that the cells isolated from rat bone marrow not only expressed CD34, CD133 and VEGFR-2, but also co-expressed Ac-LDL and UEA-1, suggesting that we successfully isolated EPCs, which therefore provide a cytological basis for the further study of cell transplantation.

With histological staining, we verified that the USPIO-labeled EPCs were recruited to the tumor periphery on day 4-7 after EPC administration. In fact, the peripheral zone of the tumors, where the iron-positive cells were detected by histological analysis, corresponded to the hypointense regions on the T2* map on the MRI images. The hypointense regions were also observed in the gliomas implanted intracranially and subcutaneously, where the magnetically labeled CD133+ cells were positive (8,22). The USPIO particles, carried by the EPCs and injected by the tail vein, were observed in

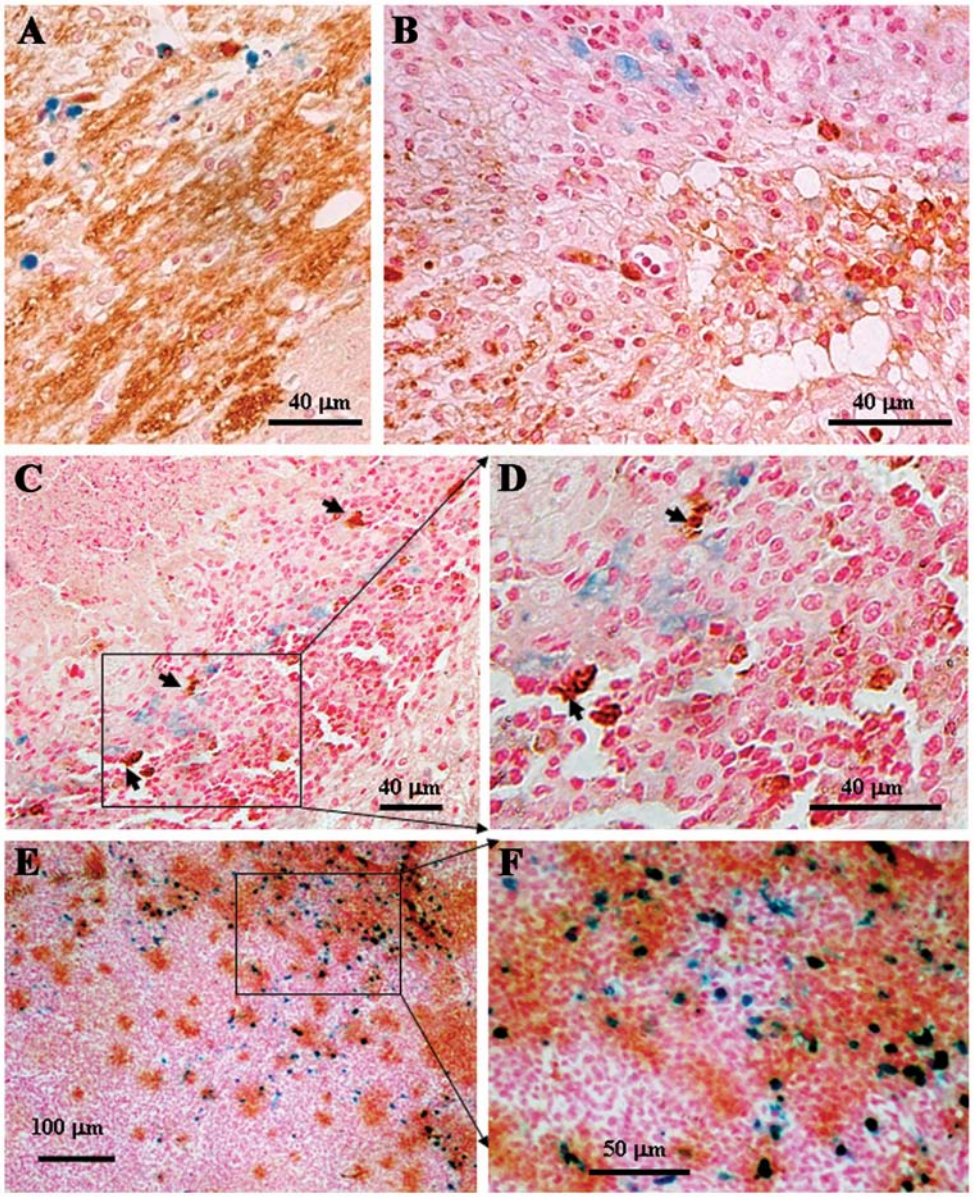

Figure 5. Identifying the transformation of EPCs in the tumor. Double labeling of CD105 (A and B), CD34 (C and D), or VEGFR2 (E and F) with iron in the tumor tissue. CD105, CD34 and VEGFR2 were detected with corresponding antibodies (yellow or brown), respectively. Prussian blue staining was used to detect the USPIO-labeled cells (blue). Scale bars are as indicated.

the tumor periphery, but not in the normal brain tissues, by MRI and histological analysis, suggesting that EPCs can home to tumors from peripheral circulating blood across the blood-brain barrier. The USPIO particles gradually dispersed into the tumor tissue from the peripheral zone along with increasing time. The profiles of the MRI images were specific for the USPIO particles, which contrasted with the images of the tumors in animals that received the unlabeled cells.

CD133, an early hematopoietic stem marker, was used as one of the surface markers for EPCs. Both CD34 and CD133 are expressed on immature cells. Mature EPCs lose CD133 during differentiation. Therefore, $CD133^+CD34^+$ EPCs are not precursors to early outgrowth EPCs (23). CD105, also termed as endoglin, is induced by hypoxia and expressed as a large population in the endothelial cells in tumors. This specific feature has made CD105 a crucial target for anticancer therapies. Our data showed that there was large number of $CD105^+$ cells in the tumor tissues, particularly in the peripheral zone of tumors, which is consistent with the findings reported by Li *et al* (24). However, only a few $CD34^+$ cells were dispersed in the tumor tissues, and few presented in vessel-like shape. Most importantly, the $VEGFR\text{-}2^+$ cells appeared in clusters and overlapped with the iron staining. The VEGFR-2-expressing cells can act as endothelial CFU precursors and may represent a more differentiated endothelial precursor (23). These findings indicate that the USPIO-labeled EPCs differentiated into endothelial cells and incorporated into the neovasculature of the tumors. In addition, glioma stem cells may trans-differentiate into EPCs when glioma cells suffer genetic aberrations (25).

MRI can detect the incorporation of magnetically labeled bone marrow-derived precursor cells (9) and cord blood-derived $AC133^+$ EPCs (26) into tumor vasculature. The bio-distribution of iron oxide-labeled human mesenchymal stem cells and fetal neural stem cells in glioblastoma has also been evalu-

ated by high resolution and contrast-enhanced MRI (27). The distribution and retention of labeled EPCs in different organs were observed using the SPECT imaging method, in which it was initially found that cell migration was observed in the lung after vein injection (28). In the present study, we used an ultra-high-field MRI (3.0 T) and the $T2^*$ map sequence to examine the signals in tumor-bearing rats. We found that the migration and incorporation of the USPIO-labeled EPCs into the tumor neovasculature were detected as a low-intensity MRI signal at the tumor periphery, as early as 24 h after EPC administration in the preformed tumors. It was observed more clearly in the $T2^*$ map. In the *in vitro* study, we also found that the $T2^*$ map was more sensitive than the T2 map. This means that the $T2^*$ map may more sensitively reflect the signal changes between different concentrations of the labeled cells.

The present study demonstrated that EPCs are able to cross the blood-brain barrier from peripheral blood and home to tumors, where they differentiate into endothelial cells, including VEGFR-2-related endothelial cells.

Acknowledgements

This research was supported by grants (30870712) to YQ.Y. and (81173074 and 91129729) to YX.S. from the National Natural Science Foundation of China.

References

1. Asahara T, Murohara T, Sullivan A, Silver M, van der Zee R, Li T, Witzenbichler B, Schatteman G and Isner JM: Isolation of putative progenitor endothelial cells for angiogenesis. Science 275: 964-967, 1997.
2. Reyes M, Dudek A, Jahagirdar B, Koodie L, Marker PH and Verfaillie CM: Origin of endothelial progenitors in human postnatal bone marrow. J Clin Invest 109: 337-346, 2002.
3. Eggermann J, Kliche S, Jarmy G, Hoffmann K, Mayr-Beyrle U, Debatin KM, Waltenberger J and Beltinger C: Endothelial progenitor cell culture and differentiation in vitro: a methodological comparison using human umbilical cord blood. Cardiovasc Res 58: 478-486, 2003.
4. Fan CL, Li Y, Gao PJ, Liu JJ, Zhang XJ and Zhu DL: Differentiation of endothelial progenitor cells from human umbilical cord blood CD 34^+ cells in vitro. Acta Pharmacol Sin 24: 212-218, 2003.
5. Wu KH, Zhou B, Lu SH, Feng B, Yang SG, Du WT, Gu DS, Han ZC and Liu YL: In vitro and in vivo differentiation of human umbilical cord derived stem cells into endothelial cells. J Cell Biochem 100: 608-616, 2007.
6. Muta M, Matsumoto G, Hiruma K, Saji S, Nakashima E and Toi M: Impact of vasculogenesis on solid tumor growth in a rat model. Oncol Rep 10: 1213-1218, 2003.
7. Sho E, Sho M, Nanjo H, Kawamura K, Masuda H and Dalman RL: Hemodynamic regulation of $CD34^+$ cell localization and differentiation in experimental aneurysms. Arterioscler Thromb Vasc Biol 24: 1916-1921, 2004.
8. Anderson SA, Glod J, Arbad AS, Noel M, Ashari P, Fine HA and Frank JA: Noninvasive MR imaging magnetically labeled stem cells to directly identify neovasculature in a glioma model. Blood 105: 420-425, 2005.
9. Arbab AS, Pandit SD, Anderson SA, Yocum GT, Bur M, Frenkel V, Khuu HM, Read EJ and Frank JA: Magnetic resonance imaging and confocal microscopy studies of magnetically labeled endothelial progenitor cells trafficking to sites of tumor angiogenesis. Stem Cells 24: 671-678, 2006.
10. Wassmann S, Werner N, Czech T and Nickenig G: Improvement of endothelial function by systemic transfusion of vascular progenitor cells. Circ Res 99: e74-e83, 2006.
11. Laing AJ, Dillon JP, Condon ET, Street JT, Wang JH, McGuinness AJ and Redmond HP: Mobilization of endothelial precursor cells: systemic vascular response to musculoskeletal trauma. J Orthop Res 25: 44-50, 2007.
12. Szmitko PE, Fedak PW, Weisel RD, Stewart DJ, Kutryk MJ and Verma S: Endothelial progenitor cells: new hope for a broken heart. Circulation 107: 3093-3100, 2003.
13. Lyden D, Hattori K, Dias S, Costa C, Blaikie P, *et al*: Impaired recruitment of bone-marrow derived endothelial and haematopoietic precursor cells blocks tumor angiogenesis and growth. Nat Med 7: 1194-1201, 2001.
14. Rafii S, Lyden D, Benezra R, Hattori K and Heissig B: Vascular and haematopoietic stem cells: Novel targets for anti-angiogenesis therapy? Nat Rev Cancer 2: 826-835, 2002.
15. Rafat N, Beck GCh, Schulte J, Tuettenberg J and Vajkoczy P: Circulating endothelial progenitor cells in malignant gliomas. J Neurosurg 112: 43-49, 2010.
16. Varma NR, Janic B, Iskander AS, Shankar A, Bhuiyan MP, Soltanian-Zadeh H, Jiang Q, Barton K, Ali MM and Arbab AS: Endothelial progenitor cells (EPCs) as gene carrier system for rat model of human glioma. PLoS One 7: e30310, 2012.
17. Corsini E, Ciusani E, Gaviani P, Silvani A, Canazza A, Bernardi G, Calatozzolo C, DiMeco F and Salmaggi A: Decrease in circulating endothelial progenitor cells in treated glioma patients. J Neurooncol 108: 123-129, 2012.
18. Soda Y, Marumoto T, Friedmann-Morvinski D, Soda M, Liu F, Michiue H, Pastorino S, Yang M, Hoffman RM, Kesari S and Verma IM: Transdifferentiation of glioblastoma cells into vascular endothelial cells. Proc Natl Acad Sci USA 108: 4274-4280, 2011.
19. Neri M, Maderna C, Cavazzin C, Deidda-Vigoriti V, Politi LS, Scotti G, Marzola P, Sbarbati A, Vescovi AL and Gritti A: Efficient in vitro labeling of human neural precursor cells with superparamagnetic iron oxide particles: relevance for in vivo cell tracking. Stem Cells 26: 505-516, 2008.
20. Hristov M, Erl W and Weber PC: Endothelial progenitor cells: isolation and characterization. Trends Cardiovasc Med 13: 201-206, 2003.
21. Yoder MC, Mead LE, Prater D, Krier TR, Mroueh KN, Li F, Krasich R, Temm CJ, Prchal JT and Ingram DA: Redefining endothelial progenitor cells via clonal analysis and hematopoietic stem/progenitor cell principals. Blood 109: 1801-1809, 2007.
22. Arbab AS, Janic B, Knight RA, Anderson SA, Pawelczyk E, Rad AM, Read EJ, Pandit SD and Frank JA: Detection of migration of locally implanted $AC133^+$ stem cells by cellular magnetic resonance imaging with histological findings. FASEB J 22: 3234-3246, 2008.
23. Povsic TJ, Zavodni KL, Vainorius E, Kherani JF, Goldschmidt-Clermont PJ and Peterson ED: Common endothelial progenitor cell assays identify discrete endothelial progenitor cell populations. Am Heart J 157: 335-344, 2009.
24. Li C, Guo B, Wilson PB, Stewart A, Byrne G, Bundred N and Kumar S: Plasma levels of soluble CD105 correlate with metastasis in patients with breast cancer. Int J Cancer 89: 122-126, 2000.
25. Zheng PP, van der Weiden M, van der Spek PJ, Vincent AJ and Kros JM: Intratumoral, not circulating, endothelial progenitor cells share genetic aberrations with glial tumor cells. J Cell Physiol 228: 1383-1390, 2013.
26. Janic B, Jafari-Khouzani K, Babajani-Feremi A, Iskander AS, Varma NR, Ali MM, Knight RA and Arbab AS: MRI tracking of FePro labeled fresh and cryopreserved long term in vitro expanded human cord blood $AC133^+$ endothelial progenitor cells in rat glioma. PLoS One 7: e37577, 2012.
27. Chaumeil MM, Gini B, Yang H, Iwanami A, Sukumar S, Ozawa T, Pieper RO, Mischel PS, James CD, Berger MS and Ronen SM: Longitudinal evaluation of MPIO-labeled stem cell biodistribution in glioblastoma using high resolution and contrast-enhanced MR imaging at 14.1 Tesla. Neuro Oncol 14: 1050-1061, 2012.
28. Varma NR, Shankar A, Iskander A, Janic B, Borin TF, Ali MM and Arbab AS: Differential biodistribution of intravenously administered endothelial progenitor and cytotoxic T-cells in rat bearing orthotopic human glioma. BMC Med Imaging 13: 17, 2013.